

# Nanoscale

Accepted Manuscript



This is an *Accepted Manuscript*, which has been through the Royal Society of Chemistry peer review process and has been accepted for publication.

*Accepted Manuscripts* are published online shortly after acceptance, before technical editing, formatting and proof reading. Using this free service, authors can make their results available to the community, in citable form, before we publish the edited article. We will replace this *Accepted Manuscript* with the edited and formatted *Advance Article* as soon as it is available.

You can find more information about *Accepted Manuscripts* in the [Information for Authors](#).

Please note that technical editing may introduce minor changes to the text and/or graphics, which may alter content. The journal's standard [Terms & Conditions](#) and the [Ethical guidelines](#) still apply. In no event shall the Royal Society of Chemistry be held responsible for any errors or omissions in this *Accepted Manuscript* or any consequences arising from the use of any information it contains.

# Silver nanowire interactions with primary human alveolar type-II epithelial cell secretions: contrasting bioreactivity with human alveolar type-I and type-II epithelial cells

*Sinbad Sweeney,<sup>a</sup> Ioannis G. Theodorou,<sup>b</sup> Marta Zambianchi,<sup>a</sup> Shu Chen,<sup>b</sup> Andrew Gow,<sup>c</sup> Stephan Schwander,<sup>d</sup> Junfeng (Jim) Zhang,<sup>e</sup> Kian Fan Chung,<sup>f</sup> Milo S.P. Shaffer,<sup>g</sup> Mary P. Ryan,<sup>b</sup> Alexandra E. Porter,<sup>b</sup> and Teresa D. Tetley<sup>a\*</sup>*

<sup>a</sup> Lung Cell Biology, Section of Pharmacology and Toxicology, Airways Disease, National Heart & Lung Institute, Imperial College London, London, UK.

<sup>b</sup> Department of Materials and London Centre for Nanotechnology, Imperial College London, London, UK.

<sup>c</sup> Department of Pharmacology and Toxicology at Rutgers University, Piscataway, New Jersey, USA.

<sup>d</sup> Department of Environmental and Occupational Health, University of Medicine and Dentistry, School of Public Health, New Jersey, USA.

<sup>e</sup> Duke Global Health Institute and Nicholas School of the Environment, Duke University, Durham, USA.

<sup>f</sup> Respiratory Medicine and Experimental Studies Unit at National Heart & Lung Institute, Imperial College London, London, UK.

<sup>g</sup> Department of Chemistry and London Centre for Nanotechnology, Imperial College London, Exhibition Road, London SW7 2AZ, UK

\*Corresponding author: Professor T D Tetley, [t.tetley@imperial.ac.uk](mailto:t.tetley@imperial.ac.uk)

**ABSTRACT**

Inhaled nanoparticles have a high deposition rate in the alveolar units of the deep lung. The alveolar epithelium is composed of type-I and type-II epithelial cells (ATI and ATII respectively) and is bathed in pulmonary surfactant. The effect of native human ATII cell secretions on nanoparticle toxicity is not known. We investigated the cellular uptake and toxicity of silver nanowires (AgNWs; 70 nm diameter, 1.5  $\mu\text{m}$  length) with human ATI-like cells (TT1), in the absence or presence of Curosurf<sup>®</sup> (a natural porcine pulmonary surfactant with a low amount of protein) or harvested primary human ATII cell secretions (HAS; containing both the complete lipid as well as the full protein complement of human pulmonary surfactant i.e. SP-A, SP-B, SP-C and SP-D). We hypothesised that Curosurf<sup>®</sup> or HAS would confer improved protection for TT1 cells, limiting the toxicity of AgNWs. In agreement with our hypothesis, HAS reduced the inflammatory and reactive oxygen species (ROS)-generating potential of AgNWs with exposed TT1 cells. For example, IL-8 release and ROS generation was reduced by 38% and 29%, respectively, resulting in similar levels to that of the non-treated controls. However in contrast to our hypothesis, Curosurf<sup>®</sup> had no effect. We found a significant reduction in AgNW uptake by TT1 cells in the presence of HAS but not Curosurf. Furthermore, we show that the SP-A and SP-D are likely to be involved in this process as they were found to be specifically bound to the AgNWs. While ATI cells appear to be protected by HAS, evidence suggested that ATII cells, despite no uptake, were vulnerable to AgNW exposure (indicated by increased IL-8 release and ROS generation and decreased intracellular SP-A levels one day post-exposure). This study provides unique findings that may be important for the study of lung epithelial-endothelial translocation of nanoparticles in general and associated toxicity within the alveolar unit.

## INTRODUCTION

Inhalation is potentially a key route of human exposure to engineered nanomaterials, from the perspective of both intentional (diagnostic and therapeutic applications) and unintentional scenarios. Understanding nanomaterial interactions with lung cells of the alveolar region is crucial, where inhaled nanoparticle deposition rate is high. The alveolar unit, at the lung periphery, forms the active gas-blood interface and is composed of alveolar type-I and type-II epithelial cells (ATI and ATII respectively) and underlying microvascular endothelial cells. ATI cells are highly attenuated, squamous cells (~200nm thick and 40 - 80  $\mu\text{m}$  in diameter; facilitating efficient gas exchange across the alveolar wall), which cover over 95% of the alveolar surface.<sup>1</sup> The cuboidal ATII cell, accounting for <5% of the total alveolar surface area, synthesises, secretes and recycles pulmonary surfactant, a lipid-protein compound that lowers surface tension at the alveolar air-liquid interface, preventing the lungs from collapsing at exhalation. Pulmonary surfactant is largely composed of phospholipids (~90% by mass) and proteins (~10% by mass)<sup>2</sup> Phosphatidylcholine predominates the phospholipid content in surfactant (~70% of total phospholipid weight), ~50% of which is saturated dipalmitoylphosphatidylcholine (DPPC), primarily responsible for surfactant's surface tension lowering capabilities.<sup>3</sup> Four functional apoproteins (surfactant protein A, B, C and D; SP-A, SP-B, SP-C and SP-D respectively) contribute to the structure and stability of pulmonary surfactant; the collectins SP-A and SP-D are also important effectors of immune recognition, opsonising foreign matter for enhanced alveolar macrophage phagocytosis.<sup>4</sup> Nanomaterials that deposit in the alveolar region following inhalation will interact firstly with pulmonary surfactant and other lung secretions before either they interact with alveolar macrophages or the alveolar epithelial

cells. It is therefore critical to understand the effects of human pulmonary surfactant when evaluating the inhalation toxicity of nanoparticles. Both DPPC and Curosurf<sup>®</sup> (a natural porcine pulmonary surfactant, purified to remove protein content) have been used to model the effect of pulmonary surfactant's lipid components on nanoparticle toxicity,<sup>5-7</sup> while SP-A and SP-D (generally isolated from rodent, porcine or human bronchoalveolar fluid) have been used to model the effect of pulmonary surfactant's immuno-protein component.<sup>8-10</sup> However, the effect of native human ATII epithelial cell secretions (which contain complete pulmonary surfactant lipids and proteins) on nanoparticle toxicity is not known.

According to the Project on Emerging Nanotechnologies (<http://www.nanotechproject.org>), nano-silver currently represents the greatest proportion of commercialised nanomaterials globally, with numerous biomedical existing applications and others in development.<sup>11</sup> In the present study, we investigated the toxicity and cellular uptake of silver nanowires (AgNWs; 70 nm diameter, 1.5  $\mu$ m length) with human alveolar epithelial type I-like cells (TT1) cells following up to 24 hours of continuous exposure, in the absence/presence of Curosurf<sup>®</sup> or harvested primary human ATII cell secretions (HAS). We also investigated the toxicity and cellular uptake of AgNWs with primary human ATII cells under the same exposure conditions as the TT1 cells. We hypothesised that both Curosurf<sup>®</sup> and HAS would confer protection for TT1 cells, limiting the toxicity of AgNWs.

## RESULTS AND DISCUSSION

### Graphical summary

A graphical summary of AgNW interactions with TT1 cells, in the absence and presence of Curosurf or HAS, is depicted in Figure 1

### **AgNW material physicochemical characteristics**

The AgNWs used in this study were synthesised in-house and thoroughly characterised as previously reported by us.<sup>12</sup> A summary of the physicochemical characteristics of these AgNWs is shown in Table 1.

### **HAS proteins binding to AgNWs**

Only 10% and 13% of the total protein available in HAS bound to 1 and 25 µg/ml AgNWs respectively, following 1 hour incubation (Figure 2 a). Interestingly, SP-A was specifically found to bind to AgNWs as indicated by both an increase in the amount of SP-A in the AgNW-containing pellet and a decrease in the amount of SP-A in the corresponding supernatant following centrifugation (the amount of SP-A in the pellet significantly increased 2.4-fold with the addition of 25 µg/ml AgNWs;  $P < 0.05$ ; Figure 2 b). SP-D was also found to bind specifically to AgNWs. Strikingly, in contrast to SP-A, the presence of SP-D in the pellet after centrifugation was entirely due to the addition of AgNWs to the HAS i.e. SP-D was not detected in the pellet of HAS alone. Following the addition of 25 µg/ml AgNWs, the amount of SP-D in the pellet had a densitometry arbitrary unit (DAU) value of  $1.51 \times 10^7$  compared to zero for HAS alone;  $P < 0.01$ ; Figure 2 b). The trend for 1 µg/ml AgNW was similar but less marked. This likely reflects the high solubility of SP-D, which does not bind to surfactant lipids and remains in the supernatant;<sup>13</sup> on incubation with AgNWs, SP-D binds to the AgNWs and hence can be located

in the AgNW-containing pellet. Scanning transmission electron microscopy with energy dispersive X-ray spectroscopy (STEM-EDX) showed that incubation with HAS does not modify the chemical composition of the AgNWs (e.g. cause sulfidation; Supplementary Figure 1). This lack of activity is in accordance with previous findings demonstrating that AgNWs are not sulfided by isolated sulphur-containing amino acids or proteins, such as cysteine or bovine serum albumin.<sup>14</sup>

### **AgNW uptake by TT1 and ATII cells**

We have previously shown that AgNW uptake by TT1 cells is rapid (~1 hour).<sup>12</sup> Thus in the present study we chose to quantify AgNW uptake at both 1 hour and 24 hours using inductively coupled plasma - optical emission spectrometry (ICP-OES), to determine whether there was further uptake over 24 hours. There was a similar uptake of AgNWs alone and with Curosurf<sup>®</sup> by TT1 cells, following 1 and 24 hour exposure (uptake values are summarised in Figure 3). Strikingly, pre-incubating the AgNWs with HAS resulted in a significant reduction in uptake; TT1 cells took up only approximately 5 and 8% of the 25 µg of the applied AgNWs, following 1 and 24 hour exposure respectively. There was no AgNW uptake by ATII cells after 1 or 24 hour exposure (Figure 3 a).

In agreement with the ICP-OES quantification data, brightfield transmission electron microscopy (BF-TEM) imaging showed that AgNWs were taken up by TT1 cells following 1 and 24 hour exposure (Figure 4a 'i', 'ii'). As shown by us previously,<sup>12</sup> some of these AgNWs enter the TT1 cells by piercing the cell membrane (Figure 4a 'i'; insert). Other AgNWs were located in endosome/lysosome-like vesicles (Figure 4a 'ii'; insert). AgNWs pre-incubated with Curosurf<sup>®</sup>

were also internalised and showed very similar uptake processes to those indicating endosomal uptake of AgNWs alone, following 1 hour and 24 hour treatment of TT1 cells (Figure 4a 'iii', 'iv'). High angle annular dark field STEM (HAADF-STEM) imaging revealed changes in the morphology of AgNWs (alone and with Curosurf®) taken up by TT1 cells (Figure 4b 'i'-'iv'). Ag(L) peaks and S(K) peaks were detected in the STEM-EDX spectra collected from the edge of the wires, showing the formation of silver sulphide (Ag<sub>2</sub>S) (Figure 4c 'i'-'iv' and Supplementary Figure 1). We have previously demonstrated that intracellular internalisation of naked AgNWs by epithelial TT1 cells results in dissolution of the AgNWs and precipitation of highly insoluble Ag<sub>2</sub>S ( $K_{sp} = 5.92 \times 10^{-51}$ ).<sup>12</sup> This Ag<sub>2</sub>S formation could act as a 'trap' for free Ag<sup>+</sup>, thus significantly limiting the short-term toxicological effects of AgNWs. In striking contrast, there was very little uptake of AgNWs that had been pre-incubated with HAS for 1 hour as measured by BF-TEM (Figure 4a 'v', 'vi') and HAADF-STEM (Figure 4c 'v', 'vi'). This low uptake of AgNWs + HAS corresponds with the ICP-OES data. After 24 hours, most of the AgNWs pre-incubated with HAS were found extracellularly to TT1 cells (Figure 4a 'vi'), close to but separated from the plasma membrane. Although pre-incubating AgNWs with HAS significantly reduced uptake of the AgNWs, they remain in close proximity to TT1 cells and there is dissolution and precipitation of Ag<sub>2</sub>S (Figure 4b 'vi' and c; discussed further below).

### **Cell viability, IL-8 release and reactive oxygen species generation**

We previously showed that AgNWs did not cause cell death nor increased the generation of reactive oxygen species in TT1 cells following 1 hour exposure.<sup>12</sup> In the present study we were interested in examining the effects of longer-term AgNW treatment and therefore chose to assess AgNW toxicity following 4 and 24 hour continuous exposure. TT1 cell viability, measured using

the MTS assay (Figure 5 a), was not significantly changed at either time interval or at any exposure concentration. One day after removal of extracellular AgNWs from the 24-hour exposure (denoted as 'Day 1 post-exposure'), TT1 cell viability significantly decreased by 15% (following 25  $\mu\text{g}/\text{ml}$  exposure;  $P < 0.05$ ). Again, there was no effect of the lower concentrations of AgNWs with TT1 cells at this time interval. ATII cell viability remained unchanged following 4 and 24 hours treatment with AgNWs and at Day 1 post-exposure (Figure 5 b). Following 24 hour treatment with 10 and 25  $\mu\text{g}/\text{ml}$  AgNWs, TT1 cell IL-8 release significantly increased by 2- and 1.8-fold respectively ( $P < 0.05$ ; Figure 6 a) and remained elevated at Day 1 post-exposure ( $P < 0.05$ ; Figure 6 a). Pre-incubation of AgNWs with Curosurf<sup>®</sup> did not affect their ability to induce IL-8 release from TT1 cells; the trend and magnitude of IL-8 release was similar following 24 hour treatment and at Day 1 post-exposure (Figure 6 a). In contrast, pre-incubation of AgNWs with HAS almost completely abolished AgNW-induced IL-8 release, both during the 24 hour exposure period and at Day 1 post-exposure (Figure 6 a). Curosurf<sup>®</sup> is a natural surfactant prepared from porcine lungs with properties similar to human pulmonary surfactant. According to the manufacturer, Curosurf<sup>®</sup> almost exclusively contains polar lipids, in particular DPPC (~50% of the total phospholipid content) together with ~1% of specific low molecular weight hydrophobic proteins SP-B and SP-C. HAS, amongst other ATII cell secretions, contains both the complete lipid as well as the full protein complement of human pulmonary surfactant (i.e. SP-A, SP-B, SP-C and SP-D). Because pre-incubation of AgNWs with Curosurf<sup>®</sup> did not reduce the material's toxicity, it is likely that the protein component (and not the lipid component) of HAS is responsible for its ability to reduce AgNW bioreactivity with TT1 cells. Vranic *et al* recently showed that Curosurf<sup>®</sup> has the ability to significantly reduce silicon dioxide uptake by human lung mucoepidermoid carcinoma cells (NCI-H292) and a murine alveolar

macrophage cell line<sup>15</sup>. In contrast, Gasser *et al* showed that Curosurf<sup>®</sup> acted to significantly increase uptake of multi-walled carbon nanotubes by human monocyte derived macrophages.<sup>16</sup> In the present study, Curosurf<sup>®</sup> had no effect on uptake or toxicity, thus the effects of Curosurf<sup>®</sup> on nanoparticle-lung cell interactions are clearly varied and depend not only on the cell type being exposed, but also on the format of the nanoparticle. Similarly, when focusing on the effects of pulmonary surfactant proteins, Ruge *et al* showed that both SP-A and SP-D increased the uptake of magnetite nanoparticles by murine alveolar macrophages,<sup>8,9</sup> while Kendall *et al* showed increased uptake of polystyrene nanoparticles by murine alveolar macrophages and dendritic cells in the presence of SP-D.<sup>10</sup> The evidence from uptake and bioreactivity studies in the present study, suggests that the protein component of HAS (e.g SP-A and SP-D) may act to reduce AgNW bioreactivity by reducing nanoparticle uptake by TT1 cells; as evidenced by the previously discussed studies by others, the binding of SP-A and SP-D to AgNWs may also act further to promote immune cell clearance. Treating ATII cells with AgNWs, for 4 or 24 hours, did not modify IL-8 release (Figure 6 b). However, at Day 1 post-exposure, ATII cell IL-8 release was significantly increased by 1.9- and 2.3-fold for 10 and 25 µg/ml AgNWs exposures, respectively ( $P < 0.05$ ; Figure 6 b). As we did not observe any uptake of AgNWs by ATII cells, we suggest that the bioreactivity seen after the recovery phase may be due to extracellular interactions (including Ag ion release) over the 24 hour exposure period, presenting as a delayed response in ATII cells. Indeed, we have previously shown that the DPPC component of pulmonary surfactant has the ability to delay the release of Ag<sup>+</sup> ions from Ag nanospheres.<sup>17</sup>

The DHE probe was used to measure the generation of reactive oxygen species (ROS; primarily superoxide anions) in TT1 and ATII cells following AgNW treatment (Figure 7). TT1 cell

superoxide levels significantly increased following 4 hour treatment with 25  $\mu\text{g/ml}$  AgNWs (1.3-fold;  $P < 0.05$ ) and following 24 hour treatment with 10 and 25  $\mu\text{g/ml}$  AgNWs (1.3- fold and 1.8-fold respectively;  $P < 0.05$ ; Figure 7 a). This increase remained at Day 1 post-exposure. As seen for IL-8 release, pre-incubation of AgNWs with Curosurf<sup>®</sup> did not affect their ability to induce ROS generation in TT1 cells; the trend and magnitude of superoxide levels was similar following 24 hour treatment and at Day 1 post-exposure (Figure 7 a). In contrast, pre-incubation of AgNWs with HAS almost completely abolished AgNW-induced ROS levels, following both the 24 hour treatment period and at Day 1 post-exposure. ATII cells are known to secrete the antioxidant, glutathione.<sup>18</sup> We measured total levels of glutathione in HAS and found that the antioxidant is present in the secretions, however it does not spin down with AgNWs following centrifugation and therefore can not contribute to the reduction in ROS that we found (Supplementary Figure 4). Treating ATII cells with AgNWs, for 4 or 24 hours, did not modify ROS levels (Figure 7 b). However, at Day 1 post-exposure, ATII cell ROS levels were significantly increased by 1.9-fold at the highest concentration of AgNW ( $P < 0.05$ ).

#### **ATII intracellular surfactant protein levels**

Because we found that ATII cells, at Day 1 post-exposure, displayed increased bioreactivity markers (i.e. IL-8 release and ROS generation) and because we found that both SP-A and SP-D bind to AgNWs, we were interested to see if this affected the intracellular stores of SP-A and SP-D. At Day 1 post-exposure, ATII cells were lysed and the intracellular levels of SP-A and SP-D were measured by Western Blotting. We determined that the intracellular amount of SP-A had significantly decreased by 57% for ATII cells that had been treated with 25  $\mu\text{g/ml}$  AgNWs; the amount of SP-A also slightly decreased, although non-significantly, for ATII cells that had been

treated with 1  $\mu\text{g/ml}$  AgNWs (Figure 8). The intracellular amount of SP-D did not significantly change for ATII cells that had been treated with 1 or 25  $\mu\text{g/ml}$  AgNWs (Figure 8). Intracellularly in ATII cells, SP-A is concentrated within endosomal-like vesicles called lamellar bodies, while SP-D is not.<sup>19</sup> Therefore, it is possible that reduced SP-A reflected a reduction in lamellar bodies. At Day 1 post-exposure, we stained and imaged the lamellar bodies in non-exposed ATII cells and ATII cells exposed to 1 or 25  $\mu\text{g/ml}$  AgNWs and found there was no marked decrease in their numbers (Supplementary Figure 3). The reduction of intracellular SP-A can, therefore, not be explained by a reduction in the number of ATII lamellar bodies and we propose that, due to SP-A binding to the AgNWs, it is unavailable for normal recycling by the ATII cells. Indeed, Zhu *et al* have shown that molecular alterations of damaged or inactivated SP-A may result in impaired ATII recycling of the protein.<sup>20</sup> Because the ATII cells are stressed at Day 1 post-exposure (indicated by increased inflammatory mediator release and ROS generation), synthesis of supplementary SP-A to replenish the lost protein, may be inhibited. Reduced functional SP-A levels are common in a number of inflammatory lung diseases; for example, impaired SP-A protein or reduced SP-A expression has been observed in a number of cystic fibrosis and asthma patients.<sup>21,22</sup>

## CONCLUSION

It has been demonstrated that the protein component of ATII cell secretions dramatically reduces the uptake and bioreactivity of AgNWs by TT1 cells. We suggest that the surfactant proteins SP-A and SP-D are likely to be involved in these mechanisms, however they need further investigation. While the evidence presented here suggests ATII secretions act to prevent ATI cell uptake and reduce the bioreactivity of AgNWs, the ATII cells themselves were found to be

vulnerable to AgNW exposure, even in the absence of AgNW uptake. The first interaction of any nanoparticle that reaches the alveoli will be with the pulmonary surfactant, including the proteins suggested here to be largely responsible for the observed reduction in AgNW uptake and bioreactivity. This study provides unique findings that are important for understanding interactions at the bio-nano interface of the alveolar unit and the impact these could have on subsequent epithelial-endothelial activity and nanoparticle translocation across the gas-liquid interface.

## EXPERIMENTAL

### Ethics Statement

The human lung tissue used in this study was surplus tissue obtained following resection for lung carcinoma. Written informed consent was obtained for all samples and the study was carried out with the approval of the Royal Brompton and Harefield Ethical Committee (Ref: 08/H0708/73).

### TT1 and ATII cell models

This laboratory has previously immortalised human ATI-like cells (derived from freshly isolated and cultured primary human ATII cells) using transduction with the catalytic subunit of telomerase (human telomerase reverse transcriptase; hTERT) and a temperature sensitive mutant of simian virus 40 large-tumour antigen.<sup>23</sup> These ATI-like (transformed type-I-like; TT1) cells, the first human ATI-like cell line to be produced, are negative for the ATII cell markers SP-C, alkaline phosphatase and thyroid transcription factor-1. Moreover, TT1s do not contain lamellar bodies. They display a thin, attenuated morphology containing vesicles, being caveolae positive. TT1 cells were cultured to confluence in either 24-well culture plates (for uptake study) or 96-well culture plates (for all other assays) using DCCM-1 tissue culture medium with 10 % FCS new-born calf serum, 0.05% G418 and 10% PSG. An initial cell seeding of  $1 \times 10^5$ /well (24 well culture plate)  $0.1 \times 10^5$ /well (96 well culture plate) yielded a confluent monolayer after 48 hours. Growth medium was replaced with serum-free DCCM-1 24 hours prior to AgNW exposure. Cells were incubated in humidified 5% CO<sub>2</sub>/95% air at 37°C.

Primary human ATII cells were isolated from human lung of grossly normal appearance obtained following resection for lung carcinoma, as described by Witherden and Tetley.<sup>24</sup> Cells were isolated from a minimum of three subjects per experiment, with a total of fifteen subjects used in this study. Briefly, lung tissue sections were perfused by injection of 0.15 M sterile sodium chloride saline solution until the draining lavage ran clear and the cell count was  $< 1 \times 10^4$  cells/ml. The tissue was then perfused with trypsin (0.25% in Hanks balanced salt solution) and incubating at 37°C for 45 minutes; trypsin was replaced twice during the incubation period. The tissue was then finely chopped in the presence of newborn calf serum (NCS), shaken for five minutes with DNase (250 µg/ml) at room temperature and passed through a 400µm filter followed by a 40 µm filter to remove large tissue debris. The cell-containing filtrate was then centrifuged at 1300 rpm for 10 minutes and the resulting pellet was re-suspended in DCCM-1 culture medium containing 50 µg/ml DNase. Cells were then incubated in tissue culture flasks for two hours (humidified incubator, 5% CO<sub>2</sub>/95% air at 37°C) to allow differential adherence and removal of contaminating mononuclear cells. Non-adherent ATII cells were removed after 2 hours and the cell suspension was centrifuged at 1300 rpm for 10 minutes. The resulting pellet was re-suspended in a DCCM-1 culture medium containing 10%NCS and 1% PSG and cells were seeded on 96 well culture plates at  $0.1 \times 10^6$  cells/well or 24 well culture plates at  $0.5 \times 10^6$  cells/well. The 96 well culture plates were pre-coated with 50 µl of 1% PureCol collagen solution (Leimuiden, Netherlands; Type I collagen) and allowed to air dry. Cells reached confluence after 48 hours. These cells have been thoroughly characterised using electron microscopy, which shows that the cells are cuboidal in morphology, have surfactant-containing

lamellar bodies, tight junctions and microvilli. Furthermore they stain positively for the ATII cell marker alkaline phosphatase and express surfactant proteins A and C and maintain their phenotype for up to six days.<sup>24,25</sup>

#### **AgNWs and preparation of Curosurf<sup>®</sup> or HAS pre-incubated AgNWs**

PVP-capped nanowires were synthesised and thoroughly characterised as previously described.<sup>12</sup> Curosurf<sup>®</sup>, a natural pulmonary surfactant prepared from porcine lungs with properties similar to human pulmonary surfactant (but lacking SP-A and SP-D), was kindly donated by Chiesi Pharmaceuticals (Cheadle UK). Harvested primary human ATII cell secretions (HAS) were prepared by first culturing primary human ATII cells to confluence in 24 well plates. Because pulmonary surfactant lies in very close proximity to the cells, we removed 900µl (of the 1ml total culture medium) to waste, leaving the remaining 100µl (containing the pulmonary surfactant and other ATII cell secretions) undisturbed. The cultures were then rinsed with RPMI 1640 culture medium and the HAS-containing rinses were pooled. Following this, no further processing of the HAS was performed. AgNWs were incubated (at room temperature and with agitation for 1 hour) with a 1:1000 dilution of Curosurf<sup>®</sup> (in RPMI 1640 culture medium) or undiluted HAS. The incubated AgNWs were then centrifuged at 10000 x g for 10 mins, the pellet (which contains the AgNWs and ATII cell surfactant secretions) was washed twice by suspension in PBS followed by centrifuging again at 10000 x g for 10 mins. Following washing, the pre-incubated AgNWs were suspended in RPMI 1640 culture medium, ready for cell exposure. The AgNWs alone sample was prepared exactly the same as the pre-incubated, except Curosurf<sup>®</sup>/HAS was substituted with RPMI 1640 culture medium.

### **TT1 and ATII treatment with AgNWs**

TT1 cells were treated with AgNWs (alone or with Curosurf<sup>®</sup> or HAS) at concentrations ranging from 0.1 - 25  $\mu\text{g/ml}$  (prepared in RPMI 1640 culture medium). The use of RPMI cell culture medium ensured that the AgNWs did not transform to Ag<sub>2</sub>S in the cell culture medium before any interactions with TT1 or ATII cells<sup>14</sup>. ATII cells were treated with AgNWs (alone) at concentrations ranging from 1 - 25  $\mu\text{g/ml}$  (prepared in RPMI 1640 culture medium). Both TT1 and ATII cells were treated for 4 and 24 hours after which conditioned medium containing extracellular AgNWs, was removed. Cells were washed three times with phosphate buffered saline (PBS) and fresh RPMI 1640 culture medium was added for a further 24 hours to determine the bioreactivity status of the cells one day post-exposure.

### **ICP-OES and Transmission Electron Microscopy analysis of AgNW uptake**

#### **Quantification of Ag in culture medium and cells**

To quantify the amount of AgNWs taken up by TT1 and ATII cells, TT1 cells were treated with AgNWs (alone or + Curosurf<sup>®</sup> or HAS) and ATII cells were treated with AgNWs (alone); the total amount of AgNWs added to TT1 or ATII cells for the uptake study was 25  $\mu\text{g}$  (i.e. 1 ml of a 25  $\mu\text{g/ml}$  concentration of AgNWs, prepared in RPMI 1640 culture medium, was used). Both TT1 and ATII cells were exposed for 1 and 24 hours, after which the treatments were removed. The cells were rinsed three times with 1 mL of fresh RPMI 1640 culture medium. The initial treatments and subsequent washes, containing the extracellular AgNWs, were stored at -21 °C until further processing. Cells were scraped with 1 ml of fresh RPMI 1640 medium and stored at -21 °C. Each experiment was repeated three times. The intracellular and extracellular amounts of Ag were determined by inductively coupled plasma optical emission spectrometry (ICP-OES)

(Thermo Scientific, UK) with a silver detection limit of 0.6 ppb, following acid digestion. Digestion procedures using only nitric acid (HNO<sub>3</sub>) have been shown to produce inaccurate results for Ag analyses, whereas digestions based on mixtures of nitric and hydrochloric (HCl) acids lead to high Ag recovery rates <sup>26</sup>. Therefore, the cell pellets and 400 µL aliquots of the extracellular medium samples were digested with 5 mL of a 1:3 mixture of HNO<sub>3</sub> (69%) and HCl (37%) overnight. The samples were diluted 10 times in ultrapure water (Milli-Q), yielding clear digest solutions, and analysed by ICP-OES.

### **Transmission Electron Microscopy**

Following the same treatment as described in the Quantification of Ag in culture media and cells, cells were rinsed with fresh RPMI 1640 culture medium and then fixed in 2.5% glutaraldehyde in 0.1M PIPES buffer, pH 7.2 for 1 h at 4°C. The fixatives were removed by washing the cells with 0.1 M PIPES buffer times. Cells were scraped, transferred to 1.5 mL Eppendorf tubes and centrifuged at 1000 g for 20 minutes to obtain cell pellets. The cell pellets were dehydrated in graded solutions of ethanol (50%, 70%, 95%, and 100%), for 5 minutes three times in each, and then washed three times, for 10 minutes each, in acetonitrile (Sigma). After dehydration, samples were progressively infiltrated with a Quetol-based resin, produced by combining 8.75 g quetol, 13.75 g nonenyl succinic anhydride, 2.5 g methyl acid anhydride, and 0.62 g benzyl dimethylamine (all from Agar Scientific). Samples were infiltrated in a 50% resin:acetonitrile solution for 2 h, in a 75% resin:acetonitrile solution overnight and in 100% resin for 4 days, with fresh resin being replaced daily. The embedded samples were cured at 60 °C for 24 h. Thin sections (90 nm) were cut from the resin blocks directly into a water bath using an ultramicrotome and a diamond knife with a wedge angle of 35°. Sections were immediately

collected on bare, 300 mesh copper TEM grids (Agar Scientific), dried and stored under vacuum until TEM analysis. No heavy metal staining process was used, as osmium tetroxide and potassium ferricyanide have been shown to cause substantial changes in the morphology and chemistry of AgNWs.<sup>14</sup> Bright field transmission electron microscopy (TEM) imaging was performed on a JEOL 2000 microscope operated at 80 kV. High Resolution Transmission Electron Microscopy (HRTEM) and Scanning Transmission Electron Microscopy (STEM) was performed at 80 kV on a FEI Titan 80–300 TEM/STEM, fitted with a Cs (image) corrector and a SiLi Energy Dispersive X-Ray (EDX) spectrometer (EDAX, Leicester UK). HRTEM and HAADF STEM-EDX analyses were performed on non-stained samples. STEM experiments were performed with a convergence semi-angle of 14 mrad and inner and outer HAADF collection angles of 49 and 239 mrad, respectively. The probe diameter was <0.5 nm.

### Cell viability

MTS is a tetrazolium compound, 3-(4,5-dimethylthiazol-2-yl)-5-(3-carboxymethoxyphenyl)-2-(4-sulfophenyl)-2H-tetrazolium that can be reduced by dehydrogenase enzymes within living cells demonstrating cellular metabolic activity and cell viability. Such reduction in the presence of an electron coupling reagent, phenazine ethosulfate (MPS), results in the production of formazan product that is soluble in tissue culture medium and the absorbance of this formazan product can be measured using spectrophotometer. TT1 or ATII cells were seeded on 96-well plates as described above. Following 4 and 24 hours treatment with AgNWs (alone) and at the recovery time point, TT1 or ATII cells were rinsed with PBS and incubated with RPMI 1640 culture medium containing the MTS reagent according to the manufacture's protocol for 45 mins (CellTiter 96® AQueous One Solution Assay, Promega, USA). The absorbance of formazan

product in the culture medium was then read using a spectrophotometer at a wavelength of 490nm.

### **Measurement of inflammatory mediator release**

TT1 or ATII cells were seeded on 96-well plates as described above. Following 4 and 24 hours treatment with AgNWs (alone or + Curosurf<sup>®</sup> or HAS) and at the recovery time point, TT1 or ATII cell mediator-conditioned medium from was assayed for concentrations of the inflammatory chemokine, human IL-8, using sandwich enzyme-linked immunosorbent assays (ELISA). The assays were performed using DuoSet<sup>®</sup> antibody kits and according to the manufacturer's directions (R&D systems, USA).

### **Generation of reactive oxygen species**

TT1 or ATII cells were seeded on 96-well plates (black, with a clear bottom) as described above. Following 4 and 24 hours treatment with AgNWs (alone or + Curosurf<sup>®</sup> or HAS) and at the recovery time point, intracellular TT1 or ATII cell reactive oxygen species (ROS) was detected by measuring the oxidation of florescent dihydroethidium (DHE). DHE is readily permeable to cells and is oxidized by ROS, primarily superoxide, to yield ethidium. Ethidium subsequently binds to DNA, which produces a detectable red fluorescence. In the present study, ROS production was measured with the DHE probe using a variation of the protocol derived from Castilho *et al.*<sup>27</sup> At each measurement point, cells were washed three times with PBS and incubated with 100  $\mu$ l RPMI 1640 culture medium containing 10 $\mu$ M DHE (Invitrogen, Paisley UK) in RPMI 1640 culture medium for 30 minutes. At the end of DHE incubation, AMs were washed twice to remove extracellular probe and read in a fluorescence plate reader at an EX/EM of 485/595nm.

**Measurement of total HAS protein and SP-A/SP-D protein binding to AgNWs**

HAS alone or HAS with 1 or 25  $\mu\text{g/ml}$  AgNWs (incubated at room temperature and with agitation for 1 hour) was centrifuged at 10000 x g for 10 mins and the total protein content in the respective supernatants was measured using the Bradford assay. Total protein binding to 1 or 25  $\mu\text{g/ml}$  AgNWs was determined by subtracting the supernatant total protein value for HAS with 1 or 25  $\mu\text{g/ml}$  AgNWs from the supernatant total protein value for HAS alone. The amount of SP-A and SP-D specifically bound to 1 or 25  $\mu\text{g/ml}$  AgNWs was also measured. Briefly, following 1 hour incubation (at room temperature with agitation) and centrifugation at 10000 x g for 10 mins, AgNWs in the pellet were washed with three rounds of 10000 x g pelleting and PBS re-suspension; protein bound to AgNWs was removed by addition of lithium dodecyl sulfate (LDS) and denaturing at 100°C for 5 minutes. The amount of SP-A and SP-D in these samples was then determined by Western Blotting (as described below for ‘ATII intercellular SP-A/SP-D protein levels’). The amount of SP-A and SP-D in the respective supernatants of these washes was also measured by Western Blotting.

**Measurement of ATII intercellular SP-A/SP-D protein levels**

After a post-exposure recovery period, ATII cells were lysed using Cell Lytic M (with protease inhibitor cocktail), incubated on ice for 30min and then centrifuged at 3000g for 20min at 4°C. Protein concentrations from ATII extracts were determined using Bradford Reagent. Equal volume of samples (mixed with 4X NuPAGE LDS sample loading buffer and 10X NuPAGE sample reducing agent, then boiled at 100°C) were loaded into NuPage 4-12% gels and electrophoretically separated using sodium dodecylsulphate-polyacrylamide gel electrophoresis (SDS-PAGE). Following gel electrophoresis, gels were rinsed in distilled water then transferred to the nitrocellulose membrane using the i-Blot™ Dry Blotting System (Invitrogen, UK). SP-A and SP-D protein on this membrane was then detected using the anti-human SP-A antibody, ab51891, and the anti-human SP-D antibody, ab97849 (both from Abcam, Cambridge, UK). SP-A and SP-D protein bands were imaged using Ultraviolet Transilluminator GelDoc-It and densitometric quantification was performed using Visionworks.

### Statistical analyses

Data from viability, inflammatory mediator release, ROS generation and ATII intracellular levels of SP-A and SP-D experiments is presented as the mean  $\pm$  standard error (where three independent experiments were performed using three separate TT1 passage generations and where four independent experiments were performed using five separate donor tissues for ATII studies). Significant differences in AgNW (dose or +/- Curosurf®) treatment on cell viability, inflammatory mediator release, ROS generation and ATII intracellular levels of SP-A and SP-D were determined using a parametric one-way analysis of variance with Bonferroni comparisons (for TT1 cell line experiments) and using a non-parametric Kruskal–Wallis test followed by

a Mann–Whitney test where appropriate (for ATII cell experiments). In all analyses, a P value  $<0.05$  was considered significant.

**Acknowledgments:**

This work was funded by a grant from the NIEHS (grant number U19ES019536). AP Acknowledges an individual ERC starting grant (Project number 257182) for additional support for AP and SC. We would like to thank Richard Blackwell and Daniella Lindsay of Chiesi Pharmaceuticals, UK for arranging the kind donation of Curosurf<sup>®</sup> to this study.

## FIGURES AND TABLES

**Table 1** - Summary of the physicochemical characteristics of AgNWs.

**Figure 1** - Graphical summary of AgNW interactions with TT1 cells in the absence and presence of Curosurf or HAS.

**Figure 2** - Total HAS protein and SP-A/SP-D protein binding to AgNWs. Proportion of total protein available in HAS, bound to 1 and 25  $\mu\text{g/ml}$  AgNW (A). Amount of SP-A and SP-D protein bound to 1 and 25  $\mu\text{g/ml}$  AgNW (B). The amount of SP-A or SP-D in the pellet (P) and the amount of SP-A or SP-D in the corresponding supernatant (S) is shown following centrifugation, in the absence and presence of AgNWs.

**Figure 3** - ICP-OES quantification of TT1 intracellular and extracellular AgNWs following 1 hour and 24 hour treatment. **(A)** TT1 cells took up approximately 53% of the 25  $\mu\text{g}$  of AgNWs applied, following 1 hour exposure, and 66% of the 25  $\mu\text{g}$  of AgNWs applied, following 24 hour exposure. Pre-incubating the AgNWs with Curosurf<sup>®</sup> resulted in a slightly higher uptake; TT1 cells took up approximately 58% of the 25  $\mu\text{g}$  of AgNWs applied, following 1 hour exposure, and 84% of the 25  $\mu\text{g}$  of AgNWs applied, following 24 hour exposure. The amount of AgNWs quantified extracellularly and the total amount of AgNWs recovered (intra- + extracellularly) is shown in **B** and **C**.

**Figure 4** - **(A)** BF-TEM imaging of AgNWs uptake by TT1 cells. N = nucleus, C = cytoplasm, E/L = endosome/lysosome, ES extracellular space. Scale bars differ and lengths are specified on each respective image. **(B)** HAADF-STEM images of TT1 epithelial cells incubated with AgNWs alone (i-ii), AgNWs with Curosurf (iii-iv) or AgNWs with HAS (v-vi; note that image 'vi' is taken at higher magnification than images i-v) for 1 and 24 hours. The images show changes in the morphology of AgNWs after their interaction with TT1 cells. The inserts show magnifications of the boxed areas in the respective images. Scale bars differ and lengths are specified on each respective image. **(C)** STEM-EDX spectra collected from the corresponding areas 1-7 marked in Figure 4b 'i'-'vi'). The presence of S in the EDX spectra indicates that the interaction of AgNWs with TT1 cells leads to dissolution and precipitation of  $\text{Ag}_2\text{S}$ . The presence of crystalline  $\text{Ag}_2\text{S}$  was confirmed by HRTEM (Supplementary Figure 1iii).

**Figure 5** - Viability of TT1 and ATII cells

Viability of (a) TT1 and (b) ATII cells, following 4 and 24 hours treatment with AgNWs and after a post-exposure recovery period. Cell viability data is presented as a % of the non-treated (NT) control (n=3)  $\pm$  SEM; significant differences between non-treated and treated cells are indicated where \*  $P < 0.05$ .

**Figure 6** - TT1 and ATII inflammatory mediator release

IL-8 release from (a) TT1 and (b) ATII cells, following 4 and 24 hours treatment with AgNWs (alone or + Curosurf<sup>®</sup> or HAS for TT1 treatments) and after a post-exposure recovery period. Increases in IL-8 release are presented in fold change (n=3)  $\pm$  SEM; significant differences between non-treated and treated cells are indicated where \*  $P < 0.05$ .

**Figure 7** - TT1 and ATII reactive oxygen species generation

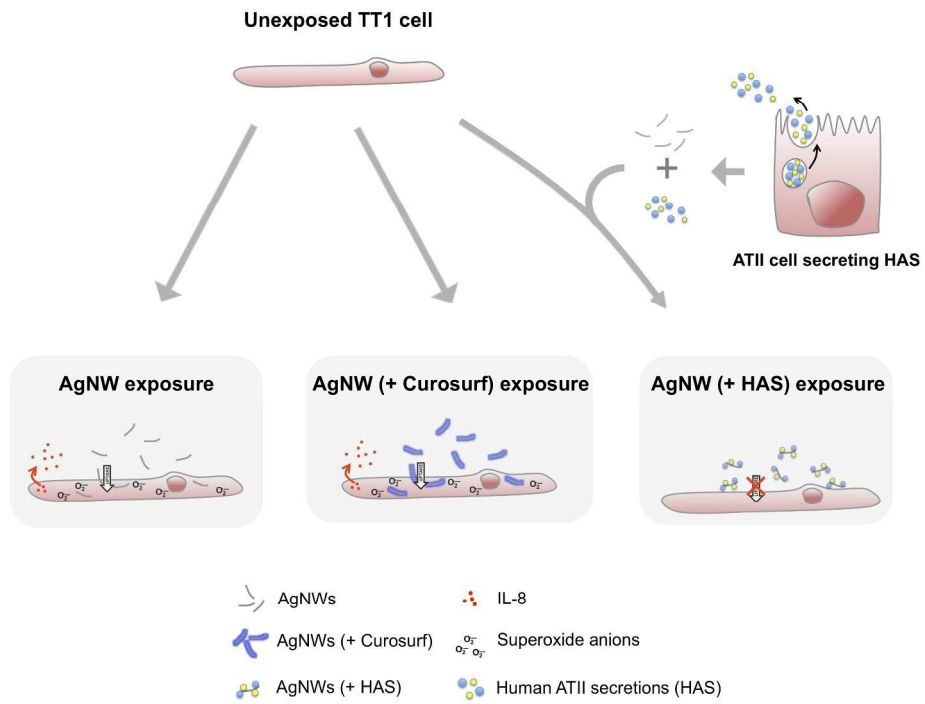
ROS levels in (a) TT1 and (b) ATII cells, following 4 and 24 hours treatment with AgNWs (alone or + Curosurf<sup>®</sup> or HAS for TT1 treatments) and after a post-exposure recovery period. Superoxide levels are presented in fluorescence units at Ex/Em: 485/595 nm (n=3)  $\pm$  SEM; significant differences between non-treated and treated cells are indicated where \*  $P < 0.05$ .

**Figure 8** - ATII intracellular levels of SP-A and SP-D at Day 1 post-exposure.

## References

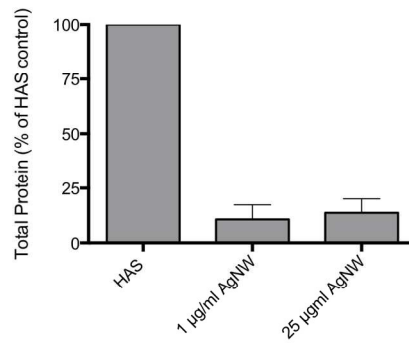
1. J. Crapo, B. Barry, P. Gehr, and M. Bachofen, *Am Rev Respir Dis*, 1982, **125**, 332–337.
2. J. Gibson, D. Geddes, U. Costabel, P. Sterk, and B. Corrin, *Respiratory Medicine*, Saunders Ltd., 3rd edn. 2003.
3. J. R. Glasser and R. K. Mallampalli, *Microbes and Infection*, 2012, **14**, 17–25.
4. Z. C. Chronos, Z. Sever-Chronos, and V. L. Shepherd, *Cellular Physiology and Biochemistry*, 2009, **25**, 13–26.
5. C. Schleh and J. M. Hohlfeld, *Inhal Toxicol*, 2009, **21 Suppl 1**, 97–103.
6. E. Herzog, H. J. Byrne, M. Davoren, A. Casey, A. Duschl, and G. J. Oostingh, *Toxicol Appl Pharmacol*, 2009, **236**, 276–281.
7. B. M. Rotoli, R. Gatti, D. Movia, M. G. Bianchi, L. Di Cristo, I. Fenoglio, F. Sonvico, E. Bergamaschi, A. Prina-Mello, and O. Bussolati, *Nanotoxicology*, 2014, 1–12.
8. C. A. Ruge, J. Kirch, O. Cañadas, M. Schneider, J. Perez-Gil, U. F. Schaefer, C. Casals, and C.-M. Lehr, *Nanomedicine: Nanotechnology, Biology and Medicine*, 2011, **7**, 690–693.
9. C. A. Ruge, U. F. Schaefer, J. Herrmann, J. Kirch, O. Cañadas, M. Echaide, J. Perez-Gil, C. Casals, R. Müller, and C.-M. Lehr, *PLoS ONE*, 2012, **7**, e40775.
10. M. Kendall, P. Ding, R.-M. Mackay, R. Deb, Z. McKenzie, K. Kendall, J. Madsen, and H. Clark, *Nanotoxicology*, 2013, **7**, 963–973.
11. Z. Huang, X. Jiang, D. Guo, and N. Gu, *J. Nanosci. Nanotech.*, 2011, **11**, 9395–9408.
12. S. Chen, A. E. Goode, S. Sweeney, I. G. Theodorou, A. J. Thorley, P. Ruenraroengsak, Y. Chang, A. Gow, S. Schwander, J. Skepper, J. J. Zhang, M. S. Shaffer, K. F. Chung, T. D. Tetley, M. P. Ryan, and A. E. Porter, *Nanoscale*, 2013, **5**, 9839.
13. A. Persson, D. Chang, K. Rust, M. Moxley, W. Longmore, and E. Crouch, *Biochemistry*, 1989, **28**, 6361–6367.
14. S. Chen, I. G. Theodorou, A. E. Goode, A. Gow, S. Schwander, J. J. Zhang, K. F. Chung, T. D. Tetley, M. S. Shaffer, M. P. Ryan, and A. E. Porter, *Environ Sci Technol*, 2013, **47**, 13813–13821.
15. S. Vranic, I. Garcia-Verdugo, C. Darnis, J.-M. Sallenave, N. Boggetto, F. Marano, S. Boland, and A. Baeza-Squiban, *Environ Sci Pollut Res*, 2013, **20**, 2761–2770.
16. M. Gasser, P. Wick, M. J. D. Clift, F. Blank, L. Diener, B. Yan, P. Gehr, H. F. Krug, and B. Rothen-Rutishauser, *Particle and Fibre Toxicology*, 2012, **9**, 17.
17. B. F. Leo, S. Chen, Y. Kyo, K.-L. Herpoldt, N. J. Terrill, I. E. Dunlop, D. S. McPhail, M. S. Shaffer, S. Schwander, A. Gow, J. Zhang, K. F. Chung, T. D. Tetley, A. E. Porter, and M. P. Ryan, *Environ Sci Technol*, 2013, **47**, 11232–11240.
18. R. J. van Klaveren, M. Demedts, and B. Nemery, *Eur Respir J*, 1997, **10**, 1392–1400.
19. R. Mason, K. Greene, and D. Voelker, *Am J Physiol Lung Cell Mol Physiol*, 1998, **275**, 1.
20. B.-L. Zhu, K. Ishida, L. Quan, M. Q. Fujita, and H. Maeda, *Legal medicine*, 2001, **3**, 134–140.
21. E. A. Van de Graaf, H. M. Jansen, R. Lutter, C. Alberts, J. Kobesen, I. J. De Vries, and T. A. Out, *J Lab Clin Med*, 1992, **120**, 252–263.
22. C. von Bredow, P. Birrer, and M. Griese, *Eur Respir J*, 2001, **17**, 716–722.
23. S. J. Kemp, A. J. Thorley, J. Gorelik, M. J. Seckl, M. J. O'Hare, A. Arcaro, Y. Korchev, P. Goldstraw, and T. D. Tetley, *Am J Respir Cell Mol Biol*, 2008, **39**, 591–597.

24. I. R. Witherden and T. D. Tetley, *Methods Mol. Med.*, 2001, **56**, 137–146.
25. I. Witherden, E. Vanden Bon, P. Goldstraw, C. Ratcliffe, U. Pastorino, and T. Tetley, *Am J Respir Cell Mol Biol*, 2004, **30**, 500–509.
26. K. D. Daskalakis, T. P. O'Connor, and E. A. Crecelius, *Environ Sci Technol*, 1997, **31**, 2303–2306.
27. S. L. Budd, R. F. Castilho, and D. G. Nicholls, *FEBS Lett.*, 1997, **415**, 21–24.

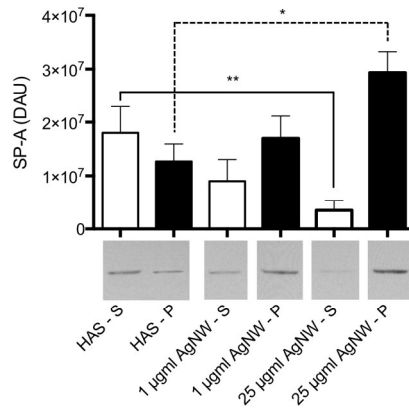
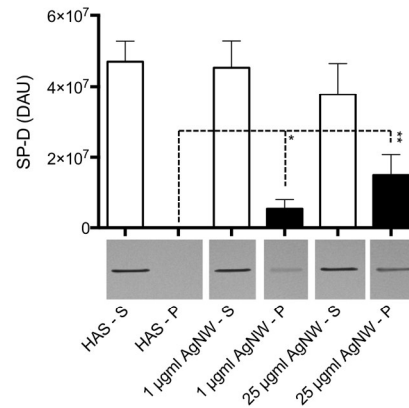


490x342mm (150 x 150 DPI)

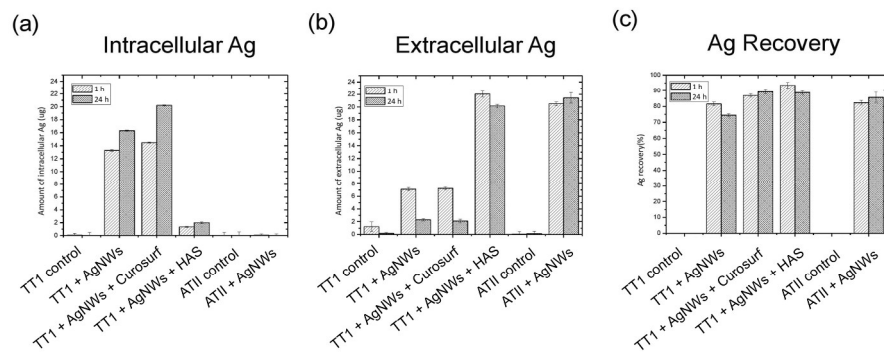
(A)

**Total protein binding to AgNWs**

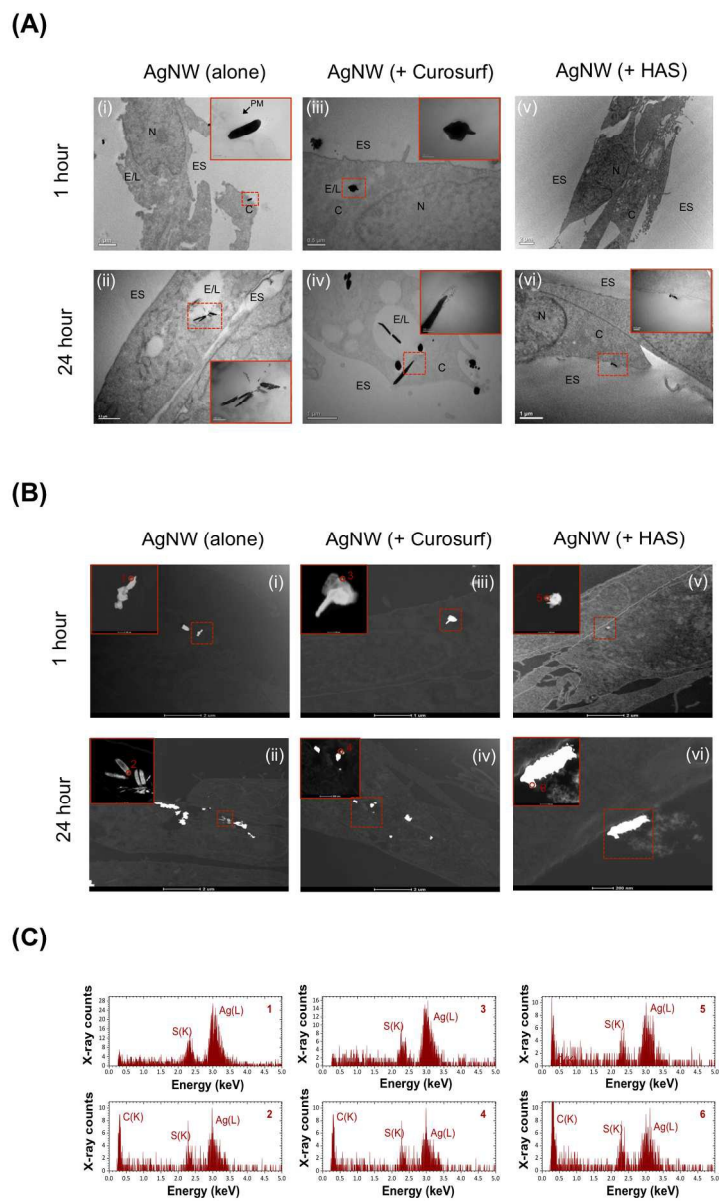
(B)

**SP-A binding to AgNWs****SP-D binding to AgNWs**

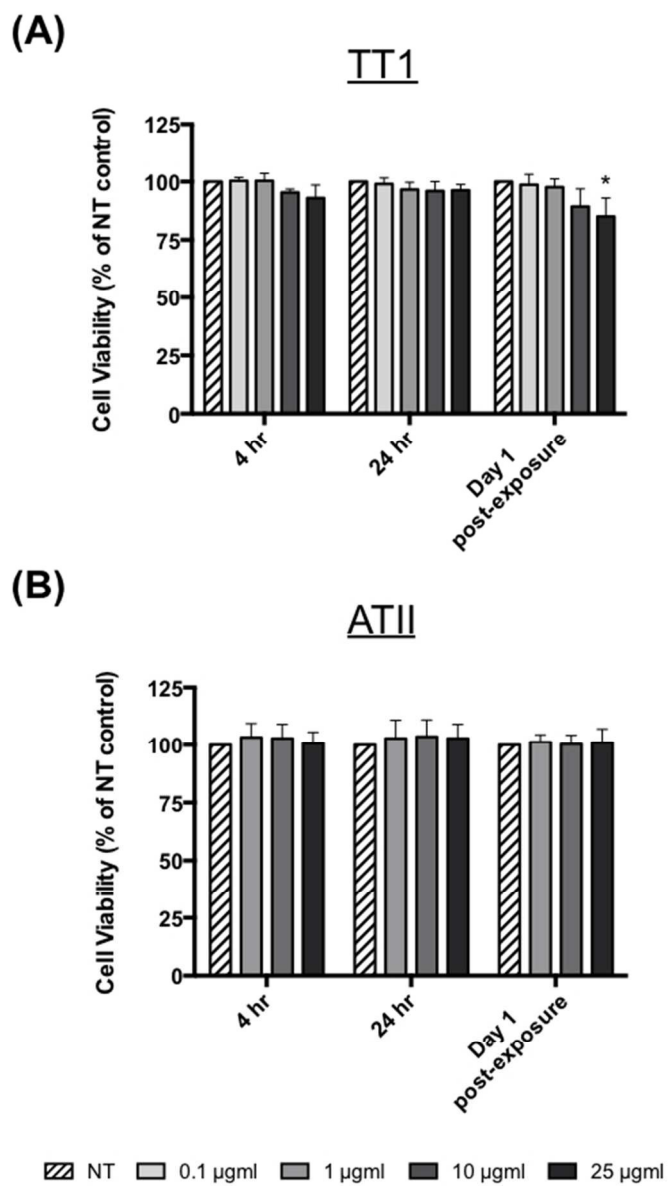
165x176mm (300 x 300 DPI)



217x80mm (300 x 300 DPI)



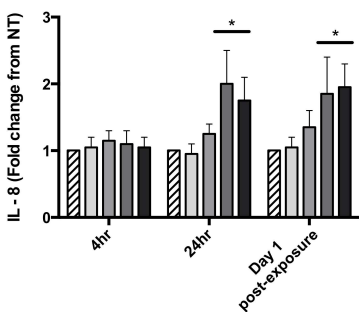
142x228mm (300 x 300 DPI)



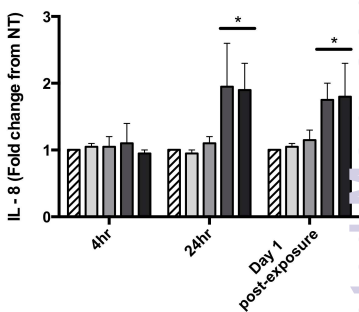
85x149mm (150 x 150 DPI)

**(A)****Nanoscale Page 32 of 35**  
**TT1**

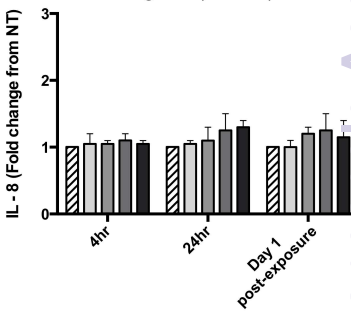
AgNW (alone)



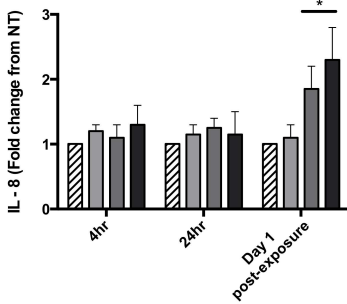
AgNW (+ Curosurf®)



AgNW (+ HAS)

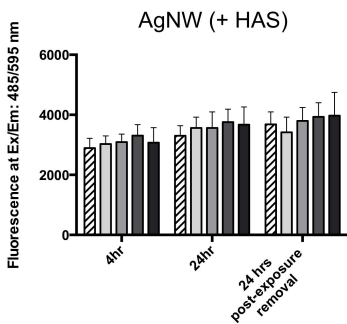
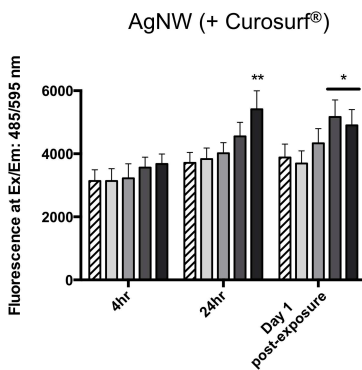
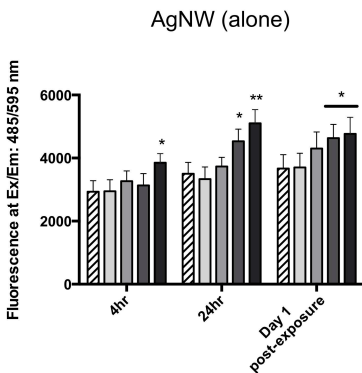
**(B)****ATII**

AgNW (alone)



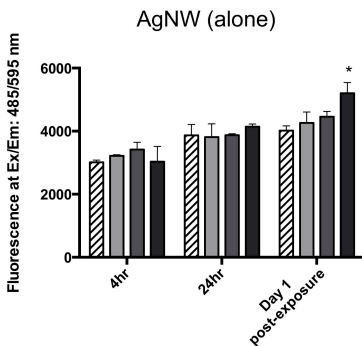
NT 0.1 µg/ml 1 µg/ml 10 µg/ml 25 µg/ml

Nanoscale Accepted Manuscript



(B)

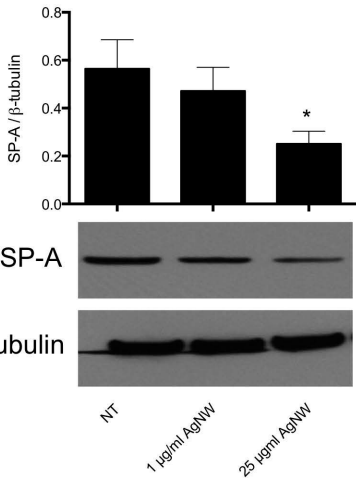
ATII



NT 0.1 µg/ml 1 µg/ml 10 µg/ml 25 µg/ml

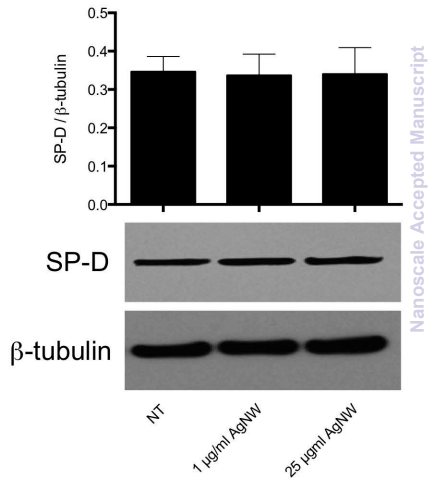
# ATII intracellular SP-A

Nanoscale



# ATII intracellular SP-D

Nanoscale



| <b>Material</b> | <b>Silver Nanowires (AgNWs)</b>  |
|-----------------|--|
| Diameter        | 72nm (36 - 108 nm)   |
| Length          | 1.5 (0.1 - 3.1 $\mu$ m)  |
| Capping Agent   | PVP (poly(vinyl pyrrolidone))<br>average molecular weight $M_w \approx 360k$ |
| Surface Charge  | $14.8 \pm 0.1$ mV  |

104x41mm (150 x 150 DPI)